

Electroactive Biofilm Serving as the Green Synthesizer and Stabilizer for *in Situ* Fabricating 3D Nanopalladium Network: An Efficient Electrocatalyst

Ya-Nan Hou,[†] Huan Liu,[§] Jing-Long Han,[‡] Wei-Wei Cai,[†] Jizhong Zhou,^{†,||} Ai-Jie Wang,^{*,†,‡} and Hao-Yi Cheng^{*,‡}

[†]State Key Laboratory of Urban Water Resource and Environment, Harbin Institute of Technology, 73 Huanghe Road, Harbin 150090, P.R. China

[‡]Key Laboratory of Environmental Biotechnology, Research Center for Eco-Environmental Sciences, Chinese Academy of Sciences, Beijing 100085, P.R. China

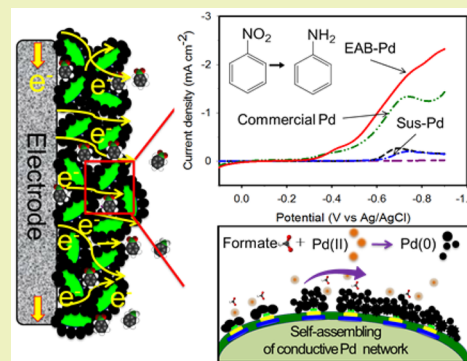
[§]Key Laboratory of Bio-Inspired Smart Interfacial Science and Technology of Ministry of Education, Beijing Key Laboratory of Bio-inspired Energy Materials and Devices, School of Chemistry and Environment, Beihang University, Beijing 100191, P.R. China

^{||}Institute for Environmental Genomics, and Department of Microbiology and Plant Biology, University of Oklahoma, Norman, Oklahoma 73019, United States

Supporting Information

ABSTRACT: Biogenetic nanopalladium (bio-Pd) has attracted increasing attention recently due to its economical and environmental friendly synthesis route. However, traditional bacteria suspensions formed palladium (Sus-Pd) is limited to be the electrochemical catalyst owing to the poor conductivity of bacterial cells. Herein, we demonstrated Pd nanoparticles, synthesized by electroactive *Geobacter* biofilm, can form a three-dimensional conductive network (EAB-Pd) that is beneficial to the electrons transfer. As a result, the EAB-Pd delivered an over 5-fold increase of current compared to the Sus-Pd in hydrogen evolution and the reductive degradation of nitro-, azo- and chloroaromatics. Superior performance of EAB-Pd was also observed in comparison with the commercial Pd catalyst. A good stability of EAB-Pd has been further confirmed under electrochemical and mechanical stresses as well as through the reuse after over 3 months of storage. This novel proposed method enables the direct electrochemical application of bio-Pd without the previous required cell carbonization and chemical binders.

KEYWORDS: Nanopalladium, Electroactive biofilm, Conductive 3D network, *In situ* fabrication, Reductive catalysis



INTRODUCTION

Synthesis of metal nanoparticles by microorganisms has recently attracted increasing attention for sustainable metal recycling and catalysts production.¹ These biologically inspired methods are performed under mild conditions without the addition of any toxic reagents, and consequently are more environmental-friendly compared to the conventional chemical methods.² Palladium (Pd) is one of the most concerned metals due to its high reductive catalytic activity, yet suffering from the growing limited supply.³

To date, the capability of producing Pd(0) has been verified in a number of bacteria when exposing the cell suspensions to Pd(II) with hydrogen or organic carbon (e.g., formate and acetate) as the electron donors. The bacteria suspensions formed Pd(0) (Sus-Pd) can be used directly as a catalyst and has shown efficient catalytic activity for reductively degrading several recalcitrant contaminants, such as nitro- and chloroaromatics.^{4–6} Nevertheless, the application of Sus-Pd is still facing several challenges including the following two aspects.

First, Sus-Pd has to be separated from the microbial incubation medium and then immobilized on the carrier to avoid losing when using as the catalyst.⁷ This makes the protocol more complex. Second, a safe and sustainable electrons donation manner is required when charging the Pd(0) to implement its catalytic activity. For this, electrode was proposed in contrast to hydrogen and other chemical reductants as the electron donation source.⁸ However, because the bacteria is poorly conductive, cell carbonization is usually performed before coating Sus-Pd onto the electrode, which would require additional equipment and energy consumption. In addition, expensive binders, such as Nafion, are inevitable to ensure a stable attachment on the electrode surface.⁹

Herein, we propose a novel procedure for Pd(0) synthesis by employing *Geobacter sulfurreducens* formed electroactive bio-

Received: March 31, 2016

Revised: July 20, 2016

Published: August 25, 2016

films (EABs), which allows the Pd synthesis, immobilization and electrochemical application at single electrode (Figure 1).

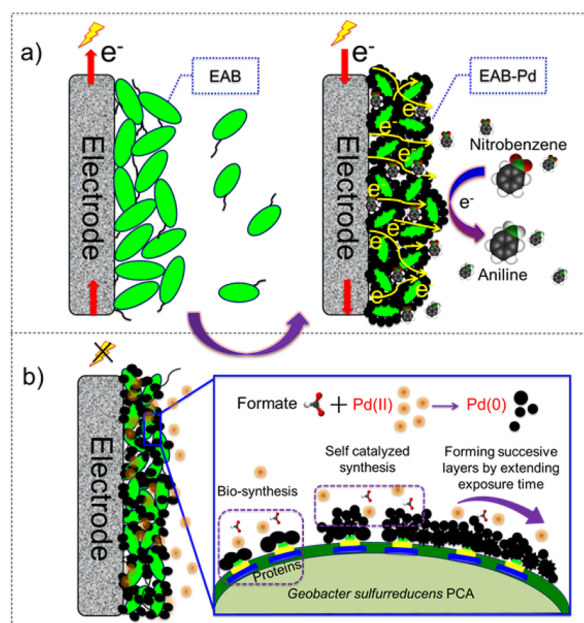


Figure 1. Schematic illustration of (a) EABs incubation and with *in situ* synthesized Pd conductive network for electrochemically catalyzing nitrobenzene reduction; (b) proposed Pd synthesis process by EABs.

The EAB formed Pd nanoparticles (EAB-Pd) were found self-assembly wrapping each bacteria cell along with the entire EAB and finally forming a three-dimensional porous network. Particularly, these cells supported Pd nanoparticles were intercontacted and constructed an electric conductive pathway from the electrode surface to the biofilm surface, which enabled the efficient electrons delivery from electrode to the entire biofilm–Pd matrix and therefore to avoid the cell carbonization as reported previously.¹⁰ The *in situ* formed 3D EAB-Pd was characterized by several microscopic and spectroscopic methods, as well as electrochemically evaluated for hydrogen evolution and the reduction of three different organic compounds that respectively represent the nitro-, azo- and chloroaromatic contaminants. For comparison, commercial submicrometer Pd catalyst and the conventional *Geobacter* suspensions produced Sus-Pd were employed as the controls. The stability of EAB-Pd was also tested under the electrochemical stress and the mechanical shear stress, respectively, as well as evaluated after over three months storage.

EXPERIMENTAL SECTION

Electrochemical Cell. The experiments including EAB incubation, EAB-Pd formation as well as the corresponding electrochemical evaluation were performed in a sealed single-chamber electrochemical cell, which equipped with a multichannel potentiostat (1030C, CH Instruments Inc., U.S.) and operated as 3-electrode mode at 30 °C. Eight identical glassy carbon electrodes (GCE, 4.0 mm in diameter) separately served as working electrodes, which shared one Ag/AgCl reference electrode and one platinum mesh (100 mm²) as the counter electrode (Figure S1c). In the case of obtaining the cross section of EAB-Pd, the working electrode was replaced by the screen printed carbon electrode (Zensor R&D, Taiwan).

EAB Preparation. *Geobacter sulfurreducens* PCA (DSM 12127) was obtained from DSMZ and precultured in PCA standard medium

according to Reguera et al.¹¹ The activated *Geobacter* suspensions (25 mL) with optical density of 0.3 to 0.5 at 600 nm were then inoculated into the electrochemical cell containing sterilized growth medium (PCA standard medium but without fumarate, 55 mL), which was subsequently fluxed with N₂/CO₂ (80:20) for 30 min. During the incubation, the working electrodes were poised at −0.20 V.

EAB-Pd Production. Once a stable electrical current output was achieved in EAB incubation stage, the medium was replaced by 60 mL fresh sterilized buffer solution (PCA standard medium without acetate and fumarate) amended with formate (25 mM) as the electron donor. A concentrated stock solution of sodium tetrachloropalladate (Na₂PdCl₄) was then added to achieve a final Pd(II) concentration of 20 mg L^{−1}. In the case of Pd(II) reduction, the working electrodes were disconnected to the potentiostat.

RESULT AND DISCUSSION

Figure 1 illustrates the *in situ* synthesis and application process of the 3D EAB-Pd network. The *G. sulfurreducens* formed EABs were prepared by posing eight identical glassy carbon electrodes (GCEs) at −0.2 V vs Ag/AgCl with acetate serving as the substrate under anaerobic condition. After 4 days of incubation, EABs with the thickness of about 9 μm covered the GCEs surface and produced the stable current of 0.412 ± 0.002 mA cm^{−2} (*n* = 8) (see Figure S1 in the Supporting Information). Subsequently, *G. sulfurreducens* EABs were exposed to Na₂PdCl₄ with formate as the electron donor for the EAB-Pd fabrication. Field-emission scanning electron microscopy (FESEM) images showed that nanoparticles with the size between 50 and 200 nm are formed around the *Geobacter* cells after exposure to Pd(II) for 3 h (Figure S2a). By extending the reaction time (e.g., at 12 h) (Figure S2b), more particles are synthesized and started to wrap the cells. At 24 h, all of the cells became well covered with the nanoparticles, which formed a three-dimensional porous network along with the EAB (Figure 2a,b,c). These cells supported nanoparticles were confirmed as the Pd(0) through energy dispersive spectrometry (EDS) (Figure S3c) and X-ray photoelectron spectroscopy (XPS) analyses (Figure 2e). FESEM images of the EAB-Pd cross section (Figure 2d) further reveal that the Pd(0) nanoparticles not only locate on the EABs surface (Figure 2a,b) but throughout the entire EABs matrix and getting to the GCEs surface. Elemental mapping analysis shows the distribution of Pd(0) is uniform from the electrode surface to the biofilm surface with the Pd content of about 80% (by weight) (Figure 2f). The final Pd loading amount of EAB-Pd at 24 h was determined as 0.604 ± 0.012 mg cm^{−2} by analyzing the carefully removed EAB-Pd from GCEs using inductively coupled plasma optical emission spectrometer (ICP-OES). The biofilm cultivation was also attempted under the condition of disconnecting the electrode to the potentiostat, in which fumarate was the sole electron acceptor. As shown in Figure S2, only a small number of bacteria colonize the electrode surface without forming a biofilm. The followed Pd synthesis was inefficient in this case. These results highlight the important role of electrode as the electron acceptor to induce the accumulation of biofilm that is active for Pd production.

Pd(0) synthesis was also carried out using alcohol (75%) inactivated *G. sulfurreducens* EABs. As shown in Figure S2d, the production of Pd nanoparticles is negligible, indicating the microbial activity of *Geobacter* plays essential role for the Pd(0) formation. This likely should be attributed to certain microbial enzymes that are capable of catalyzing the reduction of Pd(II), such as the dehydrogenase and outer-membrane cytochrome *c*.^{12,13} Additionally, abiotic Pd(II) reduction could also

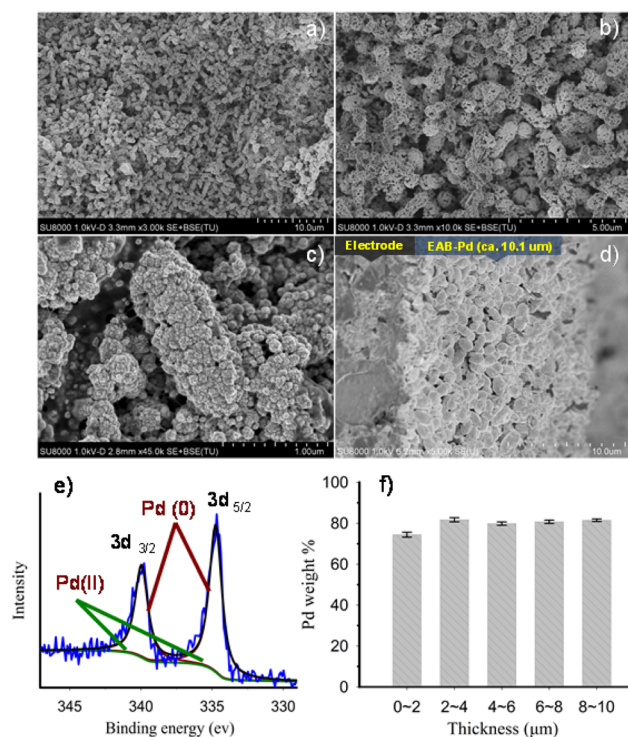


Figure 2. FESEM images of EAB-Pd after exposing to Pd(II) for 24 h. (a, b, c) Top view at 3000 \times , 10000 \times and 45000 \times magnification, respectively; (d) cross section view; (e) XPS spectra (Pd 3d region) of EAB-Pd, the Pd 3d signal is fitted to two pairs of doublets with a spin-orbit separation of 5.25 eV: Pd 3d_{3/2} (340.2 eV), Pd 3d_{5/2} (334.9 eV) and Pd 3d_{3/2} (338 eV), 3d_{5/2} (343.3 eV), which can be assigned to Pd(0) and Pd(II), respectively; (f) Pd content in EAB-Pd from the electrode side to the outer side, which was analyzed by EDS mapping.

contribute to the formation or further growth of the Pd nanoparticles, because once the biogenetic Pd(0) is formed, it would provide the nucleation sites and enable the self-catalytic Pd(II) reduction with formate as the electron donor.¹⁴ Based on these two concerns as mentioned above, the process of Pd nanoparticles formation is schematically illustrated in Figure 1b. As the control, Sus-Pd was synthesized using *G. sulfurreducens* suspension as in Tuo et al.¹⁵ According to SEM, only a few of Pd nanoparticles are formed around/on the bacteria cells in Sus-Pd (Figure S3a,b). Further analysis of EDS showed that the Pd content in Sus-Pd (13.6 ± 4.1 wt %, $n = 5$) was only 1/6 of EAB-Pd (83.8 ± 2.0 wt %, $n = 5$) (Figure S3c,d). Moreover, as that indicated by transmission electron microscopy (TEM) ultramicrotomy, the produced Pd nanoparticles in EAB-Pd are almost extracellular in contrast to the partially intercellular in Sus-Pd (Figure S4). As reported, *G. sulfurreducens* could up-regulate the expression of several outer membrane c-type cytochromes in the case of the solid electrode as the electron acceptor.¹⁶ These c-type cytochromes may then participate into the synthesis of Pd nanoparticles and therefore result in such distinct difference of Pd(0) distribution in EAB-Pd.

EAB-Pd was then electrochemically characterized through cyclic voltammetry (CV) in N₂ saturated phosphate buffer solution (PBS, pH = 7.0). As shown in Figure 3a, cathodic current starts to increase when potential is negatively swept to around -0.30 V and reaches to the maximum at -0.70 V (P_c). The onset potential of P_c is more positive than the theoretical potential of hydrogen evolution reaction (HER, ca. -0.61 V vs Ag/AgCl), in agreement with the Pd associated under potential

deposition of hydrogen (UPD H) (i.e., electrochemical adsorption/absorption of hydrogen before HER).¹⁷ The atomic H trapped in Pd was reoxidized in anodic process and therefore aroused P_a in backward scanning. As the control, CV was also performed using GCEs coated by Sus-Pd with the same Pd loading amount, but showed much poorer UPD H compared to that in EAB-Pd. Because the UPD H only occur in Pd(0) that are electrically connected to the electrode, these results clearly indicated the electron transfer efficiency between Pd(0) and electrode was dramatically boosted up in EAB-Pd, which can be well explained by its intercontacted distribution of Pd nanoparticles compared to the sporadic distribution in Sus-Pd (schematically shown in Figure 3e,f). Further evidence was supported by the significantly enlarged electrochemically active surface area (ECSA) of EAB-Pd that was shown to be over 20 times higher than that of Sus-Pd (Figure S5). Moreover, the catalytic activity of EAB-Pd for HER was also significantly enhanced with producing ca. 19.5 times higher catalytic current (poised at -0.70 V) than that in Sus-Pd (Figure 3c).

The electrochemical catalytic activity of EAB-Pd was further evaluated in the reductive degradation of recalcitrant contaminants. In the case of the nitrobenzene reduction, EAB-Pd as expected, produced much higher catalytic current than the bare GCE (ca. 10.9 times higher at -0.8 V, Figure 3b). Notably, the redox peaks observed in bare GCE CV, attributed to the intermediates (phenylhydroxylamine and nitrosobenzene) during nitrobenzene reducing to aniline,¹⁸ disappear in EAB-Pd CV (details see in SI, Figure S6). This result suggests nitrobenzene is efficiently reduced to aniline,¹⁹ consisting with the Pd catalyzed hydrogenation that has highly selectivity for transforming nitroaromatics to their corresponding amines.²⁰ In the case of Sus-Pd, the steady state current density was 7.4 times lower than that of the EAB-Pd (Figure 3d). Particularly, as that is revealed in linear sweep voltammetry (Figure 3b), the catalytic activity of Sus-Pd for nitrobenzene reduction is even inferior to the bare GCE. This deteriorated performance was previously reported in Sus-Pd involved electrochemical dehalogenation and was suggested as a result of the inhibition of less-conductive bacterial matrix.²¹ Again, this observation highlights the importance of electrical conductivity of the bacteria-Pd matrix when implementing its electrochemical catalysis. In addition to nitrobenzene, another two contaminants 4-chlorophenol (4-CP), Alizarin yellow R (AyR) were tested as the representatives of chloro- and azoaromatics, respectively. As observed in chronoamperometry (Figure S7 and Table S1), EAB-Pd still shows much higher electrochemical activity, which delivers 5-folds increase of catalytic current compared to Sus-Pd. These results suggest the improved performance of EAB-Pd is substrate independent and may be extensively perceived in the reductive degradation of contaminants.

We also compared the electrochemical catalytic activity of EAB-Pd with a commercial catalyst at the same Pd loading amount on the GCEs. As shown in Figure 3 and Table S1, EAB-Pd showed superior performance than commercial catalyst both for HER and all three contaminants reduction. This result is in agreement with the higher ECSA of EAB-Pd than that of commercial Pd (Figure S5). In addition, the porous structure of EAB-Pd may facilitate the substrates diffusion, whereas coating of commercial Pd relies on the using of Nafion binder that can decrease the pore volume of the catalyst layer (schematically shown in Figure 3g).²² Moreover, to avoid the use of chemical

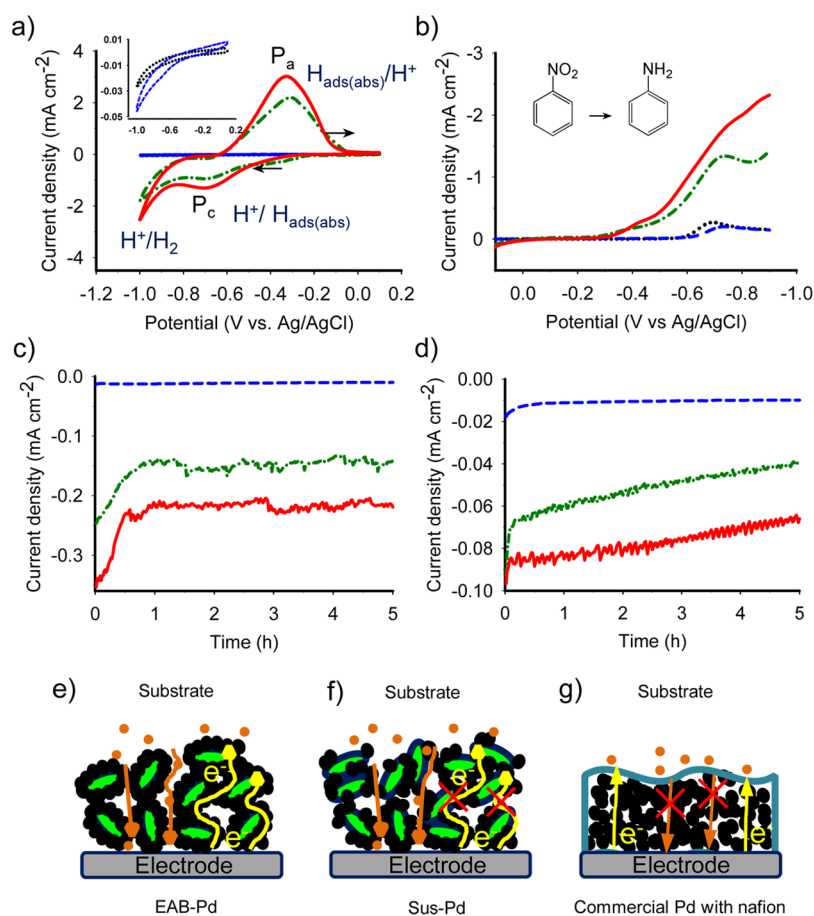


Figure 3. (a) Cyclic voltammograms of EAB-Pd (red solid), Sus-Pd (blue dash), bare (black dot) and commercial Pd (green dot dash) in PBS (50 mM). Inset: the corresponding Y-axis expansion of bare and Sus-Pd CV; (b) linear sweep voltammograms of EAB-Pd (red solid), Sus-Pd (blue dash), bare (black dot) and commercial Pd (green dot dash) in nitrobenzene (NB, 0.5 mM) amended PBS. All tests were operated under N_2 saturation condition at 30 °C with the scan rate of 10 mV s^{-1} ; (c) chronoamperometry analysis of EAB-Pd (red solid), Sus-Pd (blue dash) and commercial Pd (green dot dash) at potential of -0.7 V in PBS (50 mM) and (d) at -0.55 V in nitrobenzene (NB, 0.5 mM) amended PBS. (e, f, g) Schematic illustration of the more efficient electron transfer and substrate diffusion in EAB-Pd compared to that in Sus-Pd or commercial Pd with Nafion.

binder, the EAB based Pd synthesis procedure gain added benefits as to be more sustainable.

Finally, the stability of EAB-Pd was evaluated under electrochemical stress (i.e., 3000 cycles by CV between $+0.1$ and -1.0 V , 100 mV s^{-1}) and mechanical shear stress (i.e., electrolyte was stirred at 1000 rpm for 48 h), respectively. After EAB-Pd was exposed to the stresses, the variation of current density for HER (compared at -1.0 V , Figure 4a) and nitrobenzene reduction (compared at -0.8 V , Figure 4b) were less than 10%, indicating a good electrochemical stability was achieved in EAB-Pd. This result should be partially ascribed to the inherent filamentous structure of *Geobacter* EABs (e.g., pili or extracellular polymeric substances) that enabled a stable attachment of EAB-Pd on the electrode (Figure 4c,d). In addition, the catalytic activity of EAB-Pd was further evaluated after long time storage (100 days at 4 °C in PBS). As shown in Figure S8, the morphology of Pd network was almost the same and a comparable electrochemical performance in HER and nitrobenzene reduction were observed, which indicates the EAB-Pd is highly stable in structure and reusable.

Overall, this work provides a novel biological method for *in situ* preparing nano-Pd catalyst at the electrode. Unlike the traditional biobased method, EAB is capable of forming an electric conductive Pd network other than the sporadically

distributed Pd nanoparticles obtained in bacterial cell suspension or other biomaterial that suffers from the inefficient electrons transfer.^{23,24} This unique property allows the direct electrochemical application of the synthesized nano-Pd catalyst. Compared to the traditional electrode coating method with nano-Pd or Pd decorated carbon nanomaterial, *in situ* fabrication of nano-Pd by EAB proposed here is likely much more simple, because this novel procedure integrates the catalyst formation and immobilization in single electrode other than the separated system as is performed in a traditional way. In addition, nano-Pd immobilization in the EAB based method avoids the use of external chemical binders and is therefore more cost-effective and environmental friendly. Moreover, although many state-of-the-art Pd based catalysts have exhibited high electrochemical activity when coating on the electrode, the experiments are usually just performed using planar electrode on a very small scale.²⁵ In the case of application especially in contaminants removal, the involved electrodes are expected with more complex configuration and at larger scale, whereas the traditional coating or dipping methods may be not competent for this issue in particular of forming a uniform catalyst layer. By contrast, anode-respiring bacterium, such as *Geobacter*, is capable of “self-recognizing” the electrode surface and forming the biofilm along with the electrode.^{26,27} This

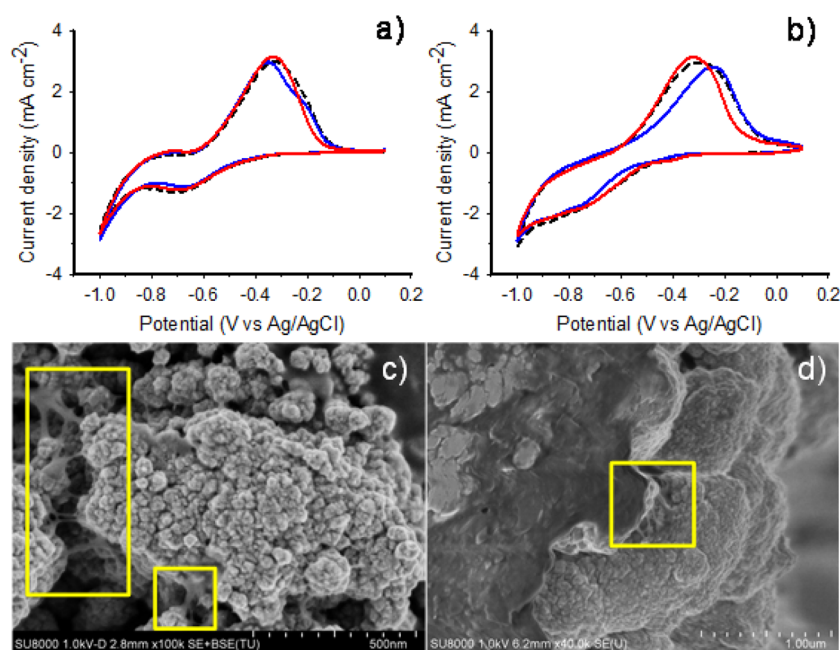


Figure 4. Cyclic voltammograms of EAB-Pd in (a) PBS and (b) nitrobenzene amended PBS before (black dash) and after respectively exposing to electrochemical stress (blue solid) and mechanical stress (red solid); (c, d) FESEM images of EAB-Pd that highlight the palladized cells are linked with each other as well as to the electrode surface by microbial produced filaments.

might allow the Pd network to be well distributed on the electrode in despite of the configuration and scale. This point is worth studying further. To be noted, the thickness of the EAB can be easily controlled by altering the cultivation time and the Pd-loading amount can be fine-tuned by changing the exposure time or concentration of Pd(II). Therefore, the Pd network fabricated based on the proposed method could be controllable and a further improvement of the catalytic performance is expected through the optimization in further. Moreover, besides *Geobacter*, some other bacteria, such as *Shewanella*, may also hold the potential to fabricate EAB-Pd because the ability of nano-Pd production as well as the electrode induced biofilm formation has been reported in this genus.^{6,28–30} As the biofilm structure and the enzymatic system involved in Pd reduction could be varied in different bacteria, optimization might also work by seeking superior bacteria and warrant further study.

CONCLUSION

We have for the first time revealed a unique three-dimensional structure of Pd(0) that can be fabrication and stabilized by *G. sulfurreducens* formed EAB. Particularly, the bacteria supported Pd nanoparticles were intercontacted and created an electrical conductive network, enabling a significant enhancement of electrochemical hydrogen evolution as well as the reductive degradation of nitro-, azo- and chloroaromatics compared to the conventional bacteria suspensions produced Pd nanoparticles with poor electrical conductivity. Superior performance of EAB-Pd was also observed in comparison with the commercial Pd catalyst. We envision that this novel EAB based Pd(0) synthesis procedure can be extended to other biogenetic metal or bimetal systems for implementing their electrochemical catalytic activity without additional chemical binders and cell carbonization.

ASSOCIATED CONTENT

Supporting Information

The Supporting Information is available free of charge on the ACS Publications website at DOI: 10.1021/acssuschemeng.6b00647.

Electrochemical active surface areas and catalytic reduction currents of EAB-Pd, Sus-Pd and commercial Pd catalyst; chronoamperogram of EAB cultivation, CLSM image of matured EAB, photo of electrochemical cell; FESEM images of EAB gradually wrapped by Pd nanoparticles with the increase of Pd(II) exposure time, FESEM images of inactivated EABs after exposing to Pd(II), FESEM images of biofilm cultivated under the condition of disconnecting the electrode to the potentiostat after Pd synthesis procedure; FESEM images and EDS mapping of Sus-Pd combined with EDS mapping of EAB-Pd for comparison; TEM ultramicrotomy images of EAB-Pd and Sus-Pd; cyclic voltammetry analysis of ECSA on EAB-Pd, Sus-Pd, commercial Pd; cyclic voltammetry analysis of nitrobenzene reduction on bare GCE and EAB-Pd; Chronoamperometry analysis of EAB-Pd, Sus-Pd, commercial Pd in 4-CP and AyR amended PBS; CV, LSV and FESEM of immersed EAB-Pd after 100 days in PBS and nitrobenzene solution (PDF).

AUTHOR INFORMATION

Corresponding Authors

*Prof. Ai-Jie Wang. E-mail: waj0578@hit.edu.cn. Fax: +86 10 62915515.

*Dr. Hao-Yi Cheng. E-mail: hycheng@rcees.ac.cn.

Notes

The authors declare no competing financial interest.

ACKNOWLEDGMENTS

Acknowledgement is made to the financial support of Natural Science Foundation of China (Grant No. 31370157, 21407164 and 21577162), National Science Foundation for Distinguished Young Scholars (Grant No. 51225802), and Hundred Talents Program of the Chinese Academy of Sciences (29BR2013001).

ABBREVIATIONS

Bio-Pd, biogenetic palladium nanoparticles; Sus-Pd, bacteria suspensions formed palladium; EAB-Pd, electroactive biofilm formed palladium; GCE, glassy carbon electrode; HER, hydrogen evolution reaction; UPD, under potential deposition; NB, nitrobenzene; 4-CP, 4-chlorophenol; AyR, Alizarin yellow R

REFERENCES

(1) Das, S. K.; Parandhaman, T.; Pentela, N.; Maidul Islam, A. K. M.; Mandal, A. B.; Mukherjee, M. Understanding the Biosynthesis and Catalytic Activity of Pd, Pt, and Ag Nanoparticles in Hydrogenation and Suzuki Coupling Reactions at the Nano-Bio Interface. *J. Phys. Chem. C* **2014**, *118* (42), 24623–24632.

(2) Huang, J.; Lin, L.; Sun, D.; Chen, H.; Yang, D.; Li, Q. Bio-inspired synthesis of metal nanomaterials and applications. *Chem. Soc. Rev.* **2015**, *44* (17), 6330–6374.

(3) Chaplin, B. P.; Reinhard, M.; Schneider, W. F.; Schuth, C.; Shapley, J. R.; Strathmann, T. J.; Werth, C. J. Critical Review of Pd-Based Catalytic Treatment of Priority Contaminants in Water. *Environ. Sci. Technol.* **2012**, *46* (7), 3655–3670.

(4) Tuo, Y.; Liu, G.; Dong, B.; Zhou, J.; Wang, A.; Wang, J.; Jin, R.; Lv, H.; Dou, Z.; Huang, W. Microbial synthesis of Pd/Fe₃O₄, Au/Fe₃O₄ and PdAu/Fe₃O₄ nanocomposites for catalytic reduction of nitroaromatic compounds. *Sci. Rep.* **2015**, *5*, 13515.

(5) Hosseinkhani, B.; Hennebel, T.; Van Nevel, S.; Verschuere, S.; Yakimov, M. M.; Cappello, S.; Blaghen, M.; Boon, N. Biogenic nanopalladium based remediation of chlorinated hydrocarbons in marine environments. *Environ. Sci. Technol.* **2014**, *48* (1), 550–557.

(6) Windt, W. D.; Aelterman, P.; Verstraete, W. Bioreductive deposition of palladium (0) nanoparticles on *Shewanella oneidensis* with catalytic activity towards reductive dechlorination of polychlorinated biphenyls. *Environ. Microbiol.* **2005**, *7* (3), 314–325.

(7) De Corte, S.; Hennebel, T.; De Gussemme, B.; Verstraete, W.; Boon, N. Bio-palladium: from metal recovery to catalytic applications. *Microb. Biotechnol.* **2012**, *5* (1), 5–17.

(8) De Gussemme, B.; Hennebel, T.; Vanhaecke, L.; Soetaert, M.; Desloover, J.; Wille, K.; Verbeken, K.; Verstraete, W.; Boon, N. Biogenic Palladium Enhances Diatrizoate Removal from Hospital Wastewater in a Microbial Electrolysis Cell. *Environ. Sci. Technol.* **2011**, *45* (13), 5737–5745.

(9) Lopez-Haro, M.; Guétaz, L.; Printemps, T.; Morin, A.; Escribano, S.; Jouneau, P. H.; Bayle-Guillemaud, P.; Chandezon, F.; Gebel, G. Three-dimensional analysis of Nafion layers in fuel cell electrodes. *Nat. Commun.* **2014**, *5*, 5229.

(10) Yates, M. D.; Cusick, R. D.; Ivanov, I.; Logan, B. E. Exoelectrogenic Biofilm as a Template for Sustainable Formation of a Catalytic Mesoporous Structure. *Biotechnol. Bioeng.* **2014**, *111* (11), 2349–2354.

(11) Reguera, G.; McCarthy, K. D.; Mehta, T.; Nicoll, J. S.; Tuominen, M. T.; Lovley, D. R. Extracellular electron transfer via microbial nanowires. *Nature* **2005**, *435* (7045), 1098–1101.

(12) Mikheenko, I. P.; Rousset, M.; Dementin, S.; Macaskie, L. E. Bioaccumulation of Palladium by *Desulfovibrio fructosivorans* Wild-Type and Hydrogenase-Deficient Strains. *Appl. Environ. Microbiol.* **2008**, *74* (19), 6144–6146.

(13) Pat-Espadas, A. M.; Razo-Flores, E.; Rangel-Mendez, J. R.; Cervantes, F. J. Direct and Quinone-Mediated Palladium Reduction by *Geobacter sulfurreducens*: Mechanisms and Modeling. *Environ. Sci. Technol.* **2014**, *48* (5), 2910–2919.

(14) Rotaru, A.-E.; Jiang, W.; Finster, K.; Skrydstrup, T.; Meyer, R. L. Non-enzymatic palladium recovery on microbial and synthetic surfaces. *Biotechnol. Bioeng.* **2012**, *109* (8), 1889–1897.

(15) Tuo, Y.; Liu, G.; Zhou, J.; Wang, A.; Wang, J.; Jin, R.; Lv, H. Microbial formation of palladium nanoparticles by *Geobacter sulfurreducens* for chromate reduction. *Bioresour. Technol.* **2013**, *133*, 606–611.

(16) Stephen, C. S.; LaBelle, E. V.; Brantley, S. L.; Bond, D. R. Abundance of the multiheme c-type cytochrome OmcB increases in outer biofilm layers of electrode-grown *Geobacter sulfurreducens*. *PLoS One* **2014**, *9* (8), e104336.

(17) Czerwiński, A.; Marassi, R.; Zamponi, S. The absorption of hydrogen and deuterium in thin palladium electrodes: Part I. Acidic solutions. *J. Electroanal. Chem. Interfacial Electrochem.* **1991**, *316* (1–2), 211–221.

(18) Li, Y.-P.; Cao, H.-B.; Liu, C.-M.; Zhang, Y. Electrochemical reduction of nitrobenzene at carbon nanotube electrode. *J. Hazard. Mater.* **2007**, *148* (1–2), 158–163.

(19) Liang, B.; Cheng, H.; Van Nostrand, J. D.; Ma, J.; Yu, H.; Kong, D.; Liu, W.; Ren, N.; Wu, L.; Wang, A.; Lee, D.-J.; Zhou, J. Microbial community structure and function of Nitrobenzene reduction biocathode in response to carbon source switchover. *Water Res.* **2014**, *54*, 137–148.

(20) Terpko, M. O.; Heck, R. F. Palladium-catalyzed triethylammonium formate reductions. 3. Selective reduction of dinitroaromatic compounds. *J. Org. Chem.* **1980**, *45* (24), 4992–4993.

(21) Hennebel, T.; Benner, J.; Clauwaert, P.; Vanhaecke, L.; Aelterman, P.; Callebaut, R.; Boon, N.; Verstraete, W. Dehalogenation of environmental pollutants in microbial electrolysis cells with biogenic palladium nanoparticles. *Biotechnol. Lett.* **2011**, *33* (1), 89–95.

(22) Yates, M. D.; Logan, B. E. Biotemplated Palladium Catalysts Can Be Stabilized on Different Support Materials. *ChemElectroChem* **2014**, *1* (11), 1867–1873.

(23) Xiong, L.; Chen, J.-J.; Huang, Y.-X.; Li, W.-W.; Xie, J.-F.; Yu, H.-Q. An oxygen reduction catalyst derived from a robust Pd-reducing bacterium. *Nano Energy* **2015**, *12*, 33–42.

(24) Devi, D. K.; Pratap, S. V.; Haritha, R.; Sivudu, K.; Radhika, P.; Sreedhar, B. Gum acacia as a facile reducing, stabilizing, and templating agent for palladium nanoparticles. *J. Appl. Polym. Sci.* **2011**, *121* (3), 1765–1773.

(25) Hu, G.; Nitze, F.; Jia, X.; Sharifi, T.; Barzegar, H. R.; Gracia-Espino, E.; Wagberg, T. Reduction free room temperature synthesis of a durable and efficient Pd/ordered mesoporous carbon composite electrocatalyst for alkaline direct alcohol fuel cell. *RSC Adv.* **2014**, *4* (2), 676–682.

(26) Lee, H.-S.; Torres, C. I.; Rittmann, B. E. Effects of substrate diffusion and anode potential on kinetic parameters for anode-respiring bacteria. *Environ. Sci. Technol.* **2009**, *43* (19), 7571–7577.

(27) Speers, A. M.; Reguera, G. Electron donors supporting growth and electroactivity of *Geobacter sulfurreducens* anode biofilms. *Appl. Environ. Microbiol.* **2012**, *78* (2), 437–444.

(28) Mertens, B.; Blothe, C.; Windey, K.; De Windt, W.; Verstraete, W. Biocatalytic dechlorination of lindane by nano-scale particles of Pd (0) deposited on *Shewanella oneidensis*. *Chemosphere* **2007**, *66* (1), 99–105.

(29) Coursolle, D.; Baron, D. B.; Bond, D. R.; Gralnick, J. A. The Mtr respiratory pathway is essential for reducing flavins and electrodes in *Shewanella oneidensis*. *J. Bacteriol.* **2010**, *192* (2), 467–474.

(30) Okamoto, A.; Nakamura, R.; Hashimoto, K. In-vivo identification of direct electron transfer from *Shewanella oneidensis* MR-1 to electrodes via outer-membrane OmcA–MtrCAB protein complexes. *Electrochim. Acta* **2011**, *56* (16), 5526–5531.